

# *Ab initio* studies of ionization potentials of hydrated hydroxide and hydronium

Charles W. Swartz and Xifan Wu

Department of Physics, Temple University, Philadelphia, Pennsylvania 19122, USA

The ionization potential distributions of hydrated hydroxide and hydronium are computed with many-body approach for electron excitations with configurations generated by *ab initio* molecular dynamics. The experimental features are well reproduced and found to be closely related to the molecular excitations. In the stable configurations, the ionization potential is mainly perturbed by water molecules within the first solvation shell. On the other hand, electron excitation is delocalized on both proton receiving and donating complex during proton transfer, which shifts the excitation energies and broadens the spectra for both hydrated ions.

PACS numbers: 61.25.Em, 71.15.Pd, 82.30.Rs, 79.60-i

The nature of the solvation structures of hydroxide ( $\text{OH}^-$ ) and hydronium ( $\text{H}_3\text{O}^+$ ) aqueous solutions are of fundamental interest. It is the prerequisite to understand the mechanism of proton transfer (PT) through the autoprolysis process in water, which is behind diverse phenomena in physics, chemistry and biology [1–7]. Photoemission spectroscopy (PES) has recently emerged as an important experimental technique in elucidating the interactions between hydrated ions and surrounding water molecules [6, 8]. In PES experiment, the ionization potential (IP) is measured by the energy required to remove an electron from the molecule with respect to the Fermi level. The state-of-art PES measurement is now able to detect the spectra signals from solvated ions which has been successfully used to determine the IPs of hydrated  $\text{OH}^-$  and  $\text{H}_3\text{O}^+$  [6]. To have an insightful understanding of the experiments, there is a critical need for theoretical modeling, at atomic scale, which can unambiguously connect the IP and its distributions to its solvation structures.

Given the disordered structures of the liquids can be simulated by *ab initio* molecular dynamics (AIMD) [10, 11], the PES spectra can be computed by the electron excitation theory such as Hedin’s GW self-energy approximation [12, 13]. However, such a theoretical approach has not yet been applied to the study of the PES spectra in ion solutions. The difficulty lies in the fact that the quasiparticle method scales unfavorably with the system size [13]. On the other hand, a proper simulation of disordered liquid structure requires a large supercell modeling. The computational burden is even more severe when it is necessary to take into account the statistical fluctuations of solvation structures both from the underlying H-bond network and more drastically, from the structural diffusion of PT. As a compromise, the computationally efficient static density functional theory (DFT) [9] or the semiclassical approximation was used [6]. However, the static DFT designed for ground state electron minimization strongly underestimates the IP as an electron excitation property [6, 9, 13]. Because of the same difficulty, the precise assignment of IPs for these hydrated ions has yet not been accurately determined.

To address the above issues, in the current work we generate the liquid structures of solvated hydroxide and hydronium in water by AIMD simulations and then compute the PES spectra within many-body formalism for electron excitation. In particular, we adopt a recently implemented methodology treating the inhomogeneous electronic screening of the medium [14–17], in which the maximally localized Wannier functions [18] are used to greatly increase the computational efficiency. The IPs of hydrated hydronium and hydroxide are determined by the real-space projection of quasiparticle density of states on these solvated ion complexes. The resulting IPs and their distribution are in quantitative agreement with experiments in both position and broadening. The IPs of hydrated ions in liquid solutions are associated with the molecular excitation, however, strongly influenced by the water molecules in the first solvation shell. During the PT, the structural diffusion results in a delocalized defect eigenstate. As a result, the IPs of hydrated ions are broadened and shift into the main feature of bulk water. To the best of our knowledge, this is the first time that GW based quasiparticle theory has been applied to the PES spectra of ion solutions. This approach will be also useful to study other important liquids.

Ion solutions are generated by two equilibrated AIMD trajectories [10] containing either one hydroxide or hydronium with 63 surrounding water molecules. A periodic cubic cell corresponding to the experimental ambient density of water is used. Both simulations are preceded by a 3 ps equilibrium run and then continued over a 25 ps time scale within the canonical ensemble. An elevated temperature of  $T = 330\text{K}$  is used, which has been found to approximately capture structural softening of H-bond in liquid water due to the quantum nuclear effect [19]. The atomic force is calculated by DFT using the PBE functional [20] with a kinetic energy cutoff of 70 Ry. Electron excitation calculations are completed using the static Coulomb hole and screened exchange (COHSEX) approach combined with electron screening effects from the inhomogeneous medium within the Hybertsen-Louie ansatz. All calculation are performed using the

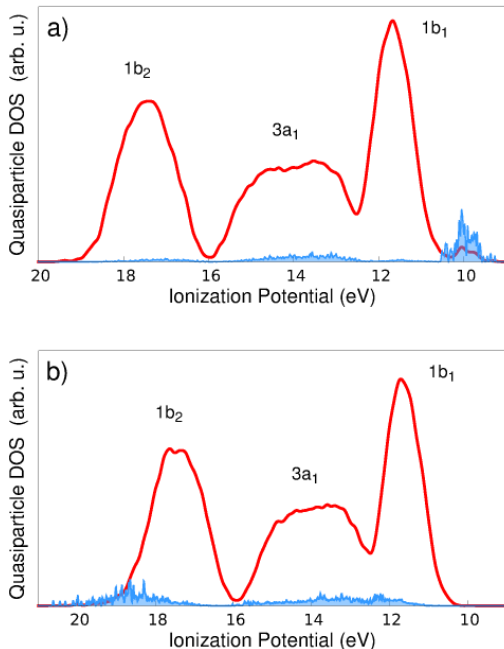


FIG. 1: (color online) Theoretical PES spectra (red line) for the (a)  $\text{OH}^-$  and (b)  $\text{H}_3\text{O}^+$  ion solutions. The shaded (blue) area indicates the IPs of hydrated  $\text{OH}^-$  and  $\text{H}_3\text{O}^+$  [22].

QUANTUM-ESPRESSO code package [21].

In Fig. 1 we present our theoretical PES spectra of both ion solutions based on quasiparticle density of states (QDOS). It can be seen that the overall PES spectra of both hydronium and hydroxide solutions are dominated by three features belonging to bulk water, which have  $1b_2$ ,  $3a_1$ , and  $1b_1$  characteristics with decreasing excitation energy as shown in Fig. 2(a), (b), and (c) respectively. The IP is associated with the valence electron excitation of solvated ion in water. Although embedded in the water solution PES spectra, it still can be identified by the realspace projection of the QDOS onto the hydrated ions in the energy range [22]. The resulting IP distributions of hydrated hydroxide and hydronium are also shown in the shaded areas of Fig. 1(a) and (b) respectively. It can be seen that the main feature of the IP of hydrated  $\text{OH}^-$  is represented by a narrow distribution, whose peak centered at 9.99 eV and close to the low energy edge of the  $1b_1$  feature of bulk water. The spectra signal is much less obvious in the  $3a_1$  region and almost absent in the  $1b_2$  region of bulk water. As far as the IP of hydrated  $\text{H}_3\text{O}^+$  is concerned, the only prominent feature is a broad peak centered at 19.01 eV close to the high energy edge of  $1b_2$  feature of bulk water. Much less signal is found in  $3a_1$  region and almost no signal is found in  $1b_1$  region of bulk water. Strikingly, current theory accurately reproduces the experimental measurement [6], in which the IPs of hydrated hydroxide and hydronium are found to be centered at  $\sim 9.2$  eV and  $\sim 20$  eV respectively. The spectra distribution of solvated hydronium

is also found to be much broader than that of hydroxide in experiment [6]. In stark contrast, the previous studies based on DFT calculations revealed that the IPs of solvated  $\text{OH}^-$  and  $\text{H}_3\text{O}^+$  were located at  $\sim 12$  eV and  $\sim 5$  eV respectively, which underestimated the experimental value over 50% [9]. This is because DFT, as a ground state theory, strongly underestimates the optical band gap properties. For a direct comparison with PES experiments, the electron excitation process can be more appropriately described by the GW self-energy approximation. We want to stress here that the IPs for both solvated ions are averaged over 100 configurations, weighted to include both PT [23] and non-PT configurations, sampled during the 25 ps equilibrium trajectory. PT configurations account for  $\sim 10\%$  of the total  $\text{OH}^-$  configurations and  $\sim 16\%$  of the  $\text{H}_3\text{O}^+$  configurations.

The accurate quasiparticle predictions now enable more precise assignment of the IPs of hydrated ions. In Fig. 2, we present the representative quasiparticle wavefunctions (QWs) for the main features, which are located close to  $1b_1$  region of bulk water for hydrated  $\text{OH}^-$  and close to  $1b_2$  region of bulk water for hydrated  $\text{H}_3\text{O}^+$ . The typical QWs of less prominent features are also shown in Fig. 2, whose energies are in the  $3a_1$  region of bulk water for both ion solutions. For comparison, the three lowest IP energy states of the  $\text{OH}^-$  and  $\text{H}_3\text{O}^+$  monomer are also presented. The similarity of the electron excitation in ion solutions and that in gas phases indicates that the IPs should be attributed to molecular ionization, however, strongly perturbed by the solvation structures of the surrounding water molecules.

Clearly, the main feature of the IP in hydrated hydroxide at 9.99 eV should be assigned to the first valence electron excitation of  $\text{OH}^-$  monomer. This is due to the resemblance of the electron excitations between the gas phase and the liquid solution. In the aqueous solution, the typical QW of the main feature is a well localized hydroxide defect state of clear lone pair character as shown in Fig. 2(g) and (i). It originates from two degenerate  $1\pi$  bonds of the  $\text{OH}^-$  monomer. The degeneracy is broken by the disordered liquid structure and results in an excitation distribution instead of one single ionization energy. It can be expected that the spectra distribution is largely dependent on the solvation structure and will be different with or without PT. In the absence of PT, current AIMD simulation finds that solvated hydroxide adopts the most stable configuration in such a way that  $\text{OH}^-$  accepts four H-bonds with the possibility of donating one [1]. The four water molecules donating H-bond are approximately in one plane. Consistently this lone pair QW is mainly localized on the  $\text{OH}^-$  itself, however, with a significant weight on the water molecules within the first solvation shell. Thus without PT, the IP is mainly affected by the fluctuating first-shell solvation structure embedded in the H-bond network of liquid water. During PT, the  $\text{OH}^-$  exchanges one proton with

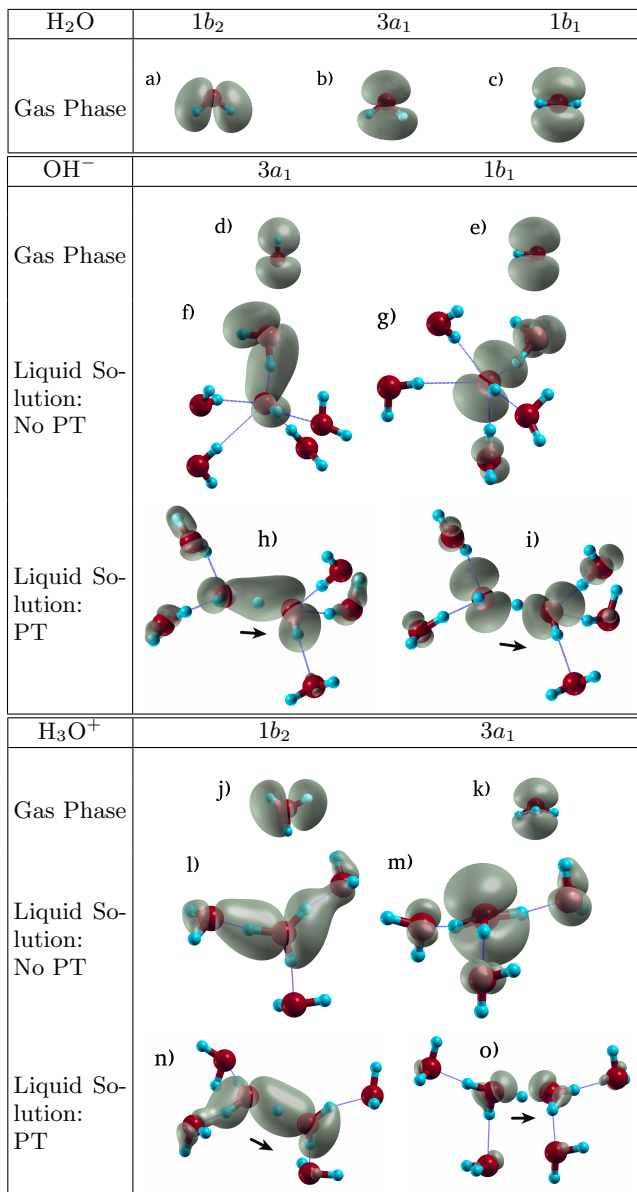


FIG. 2: (color online) QWs shown for gas phase (a)-(c) H<sub>2</sub>O, (d)-(e) OH<sup>-</sup> and (j)-(k) H<sub>3</sub>O<sup>+</sup>. Typical main feature 3a<sub>1</sub> and 1b<sub>1</sub> QWs displayed for hydrated OH<sup>-</sup> in liquid solution while (f)-(g) in a non-PT complex and (h)-(i) during a PT. Similar 1b<sub>2</sub> and 3a<sub>1</sub> QWs displayed for hydrated H<sub>3</sub>O<sup>+</sup> while (l)-(m) in the Eigen complex and (n)-(o) in the Zundel complex.

neighboring water molecule. Our current simulation indicates that the PT mechanism is consistent with the *dynamical hypercoordination* scenario proposed by Tuckerman *et al* [1]. The structural diffusion is initiated by breaking one of the four accepting H-bonds and followed by a proton exchange along the shortest H-bond. Intriguingly, the structural diffusion is accompanied by a nontrivial change in the electronic state. The lone pair QW is now localized on both proton donating and proton receiving molecules as shown in Fig. 2(i) instead of its main localization on OH<sup>-</sup> only before the PT in Fig. 2(g).

The delocalized QW facilitates its hybridization with surrounding water molecules. As a result, the IP exhibits a blue shift towards the main feature of the bulk water spectra accompanied by a broadened distribution as illustrated in Fig. 3(a).

In a similar scenario, we assign the main feature of the IP distribution of hydrated hydronium to the second valence excitation of two degenerate *p* orbitals of H<sub>3</sub>O<sup>+</sup> monomer. The degeneracy is again broken by the disordered molecular environment. Without PT, the excited QW has a similar characteristic of 1b<sub>2</sub> of liquid water and is mainly localized on the so-called Eigen complex (H<sub>3</sub>O<sup>+</sup>) as shown in Fig. 2(l). In particular, a large orbital amplitude is also found on the three water molecules along the direction of donated H-bonds by H<sub>3</sub>O<sup>+</sup>. The QW then decays rapidly to zero in the second solvation shell and beyond. As a result, the excitation is a hydronium defect state with 1b<sub>2</sub> character that is localized on the H<sub>9</sub>O<sub>4</sub><sup>+</sup> complex, which is also the so-called *strongly solvated Eigen cation* in the literature [24]. In the process of PT, the current simulation is consistent with the widely accepted Grotthus diffusion mechanism [1]. The proton exchange takes place by the interconversion between Eigen and Zundal (H<sub>5</sub>O<sub>2</sub><sup>+</sup>) complex [1]. Not surprisingly, the locality of the QW also swifts from the Eigen to the Zundal complex during PT as shown in Fig. 2(l) and (n) respectively. Interestingly, a significant weight is also found to be centered on the transferring proton connecting both the proton receiving and donating structures, which gives a unique signal for PT in the electronic structure. Similar to the PT process of hydrated OH<sup>-</sup>, the delocalized H<sub>3</sub>O<sup>+</sup> defect state is much more easily to be hybridized with solvent H<sub>2</sub>O molecules. As a result, in Fig. 3(b) we observe a red shift of the IPs into the 1b<sub>2</sub> region of bulk water which gets broadened simultaneously.

Interestingly, a comparison of the IPs between these two ion solutions reveals that the main feature of hydrated H<sub>3</sub>O<sup>+</sup> has a much broader distribution than that of OH<sup>-</sup>. We attribute it to the difference in orbital characters. For the hydrated H<sub>3</sub>O<sup>+</sup> excitation with 1b<sub>2</sub> characteristic, the covalent orbital on an OH bond is easily perturbed by the H-bond network of liquid water. On the other hand, the excitation of hydrated OH<sup>-</sup> is of lone pair character and only centered on oxygen atom which will be much less effected by the embedded H-bond network. This is also consistent with the observation that 1b<sub>1</sub> is already narrowed than 1b<sub>2</sub> peak in liquid water [25].

Besides the main features, the excitations of hydrated ions are also found in Fig. 1(a) and (b) within the 3a<sub>1</sub> region of bulk water for both solutions. However the signals are much weaker and broadly distributed. Nevertheless, the IPs of hydrated ions should still be assigned to the molecular excitation of the same 3a<sub>1</sub> symmetry, which are the second and first excitation of OH<sup>-</sup> and H<sub>3</sub>O<sup>+</sup> monomers respectively. In Fig. 4(a) and (d), we present

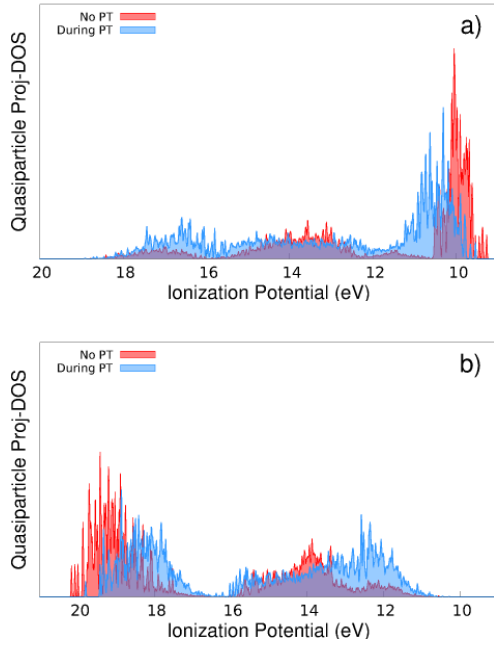


FIG. 3: (color online) Theoretical IP distributions for hydrated (a)  $\text{OH}^-$  and (b)  $\text{H}_3\text{O}^+$ . The *red* area indicates those configurations where the respective hydrated ion is not experiencing a PT ( $\delta > 0.6$  Å [26]) and the *blue* area indicates those configurations currently experiencing a PT ( $\delta \sim 0$  Å).

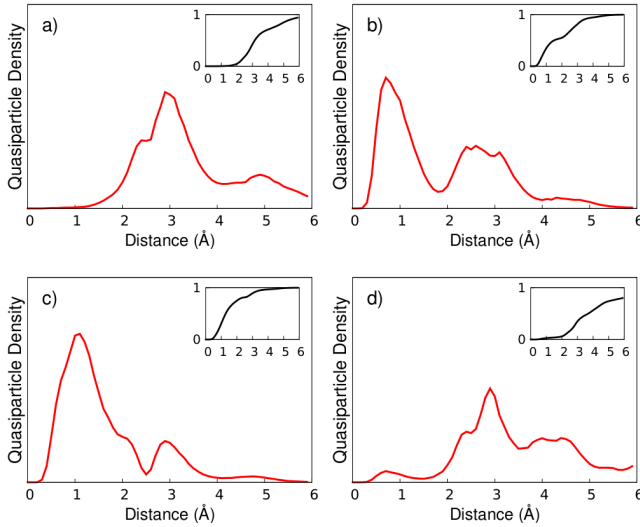


FIG. 4: Typical QW densities (arb. u.) for hydrated  $\text{OH}^-$  characteristic states, (a)  $3a_1$  and (b)  $1b_1$ , and hydrated  $\text{H}_3\text{O}^+$  characteristic states, (c)  $1b_2$  and (d)  $3a_1$ , as a function of distance from  $\text{O}^*$  [22]. Inserts show the total integrated density.

typical QW densities of  $3a_1$  excitations as a function of distance from the solvated  $\text{OH}^-$  and  $\text{H}_3\text{O}^+$  respectively. For comparison, the same quantities of the main feature are also shown in Fig. 4(b) and (c). Clearly, in both ion solutions, the less prominent IPs of  $3a_1$  character originate from relatively delocalized QWs, in which a large

orbital amplitude falls into the second solvation shell and beyond. On the contrary, QWs of the main features of both hydrated ions are strongly localized defect states within the first solvation shell. As a result, the integrated charge approaching to one electron rapidly with the increased distance away from the ions. The delocalized QWs indicate a stronger hybridization with the water solution and result in the observed broader and weaker ion excitations.

Finally, we draw our attention to the energy range where the least IP signals have been found. They are the  $1b_2$  and  $1b_1$  region of bulk water for hydrated  $\text{OH}^-$  and  $\text{H}_3\text{O}^+$  respectively. Again, this can be understood by the symmetry of electron excitation of both ions at the monomer level. The electronic configurations of  $\text{OH}^-$  and  $\text{H}_3\text{O}^+$  ions are intrinsically different from that of a single water molecule. For  $\text{OH}^-$  monomer, the three lowest allowed valence excitation are the two degenerated excitation of  $1b_1$  character, followed by one of  $3a_1$  character, in which the  $1b_2$ -like orbital in water is not allowed by symmetry. On the other hand, the three lowest valence excitation in  $\text{H}_3\text{O}^+$  ion are one with  $3a_1$  character, followed by two degenerate states with  $1b_2$  character, in which the lone pair  $1b_1$ -like orbital in water is forbidden. These symmetry restrictions are also reflected in ion solutions and result in the absence of electron excitation for hydrated ions in the above energy range.

In conclusion, the IP distributions of hydrated  $\text{OH}^-$  and  $\text{H}_3\text{O}^+$  are studied by accurate quasiparticle theory. The excitations of solvated ions can be assigned to molecular electron excitation, however, strongly perturbed by the solvation structures. Although the main features of IPs are determined by their stable configurations, the proton transfer does introduce a change of position and distributions of electron excitation in both hydrated ions. We suggest that the excitation change due to PT can be detected by isotope effect in future PES measurements performed on solvated  $\text{H}_3\text{O}^+$  and  $\text{D}_3\text{O}^+$ . Because of the quantum nuclear effect lowers the barrier of proton transfer [27], the hydrated  $\text{H}_3\text{O}^+$  will have a more broad and shifted IP distribution than that of  $\text{D}_3\text{O}^+$ . Finally we comment that the leftover mismatch between experiment and theory could be further reduced by more accurate liquid structures considering both dispersion force [28–30] and self-interaction error correction [31, 32] and by including frequency dependence of excitation beyond static GW [33, 34].

XW thanks valuable discussion with Roberto Car. This work is supported by U.S. Department of Energy under Grant No. DE-SC0008726. Computational support is provided by the National Energy Research Scientific Computing Center.

- 
- [1] D. Marx, A. Chandra, M. K. Tuckerman, *Chem. Rev.* **110**, 2174 (2010).
- [2] M. Tuckerman, A. Chandra, and D. Marx, *Acc. Chem. Res.* **39**, 151 (2006).
- [3] A. Hassanali, M. K. Prakash, H. Eshet, and M. Parrinello, *Proc. Natl. Acad. Sci.* **108**, 20410 (2011).
- [4] J. T. Hynes, *Nature* **397**, 565 (1999).
- [5] D. Asthagiri, L. Pratt, J.D. Kress, and M. Gomez, *Proc. Natl. Acad. Sci.* **101**, 19 (2004).
- [6] B. Winter, M. Faubel, I. Hertel, C. Pettenkofer, S. Bradforth, B. Jagoda-Cwiklik, L. Cwiklik, and P. Jungwirth, *J. Am. Chem. Soc.* **128**, 3864 (2006).
- [7] A. Chandra, M. Tuckerman, and D. Marx, *Phys. Rev. Lett.* **99**, 145901 (2007).
- [8] B. Winter, R. Weber, I. V. Hertel, M. Faubel, P. Jungwirth, E. C. Brown, and S. E. Bradforth, *J. Am. Chem. Soc.* **127**, 7203 (2005).
- [9] M. Tuckerman, K. Laasonen, and M. Parrinello, *J. Chem. Phys.* **103**, 150 (1995).
- [10] R. Car, and M. Parrinello, *Phys. Rev. Lett.* **55**, 2471 (1985).
- [11] P. Sit, C. Bellin, B. Barbiellini, D. Testemale, J. -L. Hazemann, T. Buslaps, N. Marzari, and A. Shukla, *Phys. Rev. B* **76**, 245413 (2007).
- [12] L. Hedin, *Phys. Rev.* **139**, A796 (1965).
- [13] G. Onida, L. Reining, and A. Rubio, *Rev. Mod. Phys.* **74**, 601 (2002).
- [14] M. S. Hybertsen and S. G. Louie, *Phys. Rev. B* **37**, 2733 (1988).
- [15] X. Wu, A. Selloni, and R. Car, *Phys. Rev. B* **79**, 085102 (2009).
- [16] W. Chen, X. Wu, and R. Car, *Phys. Rev. Lett.* **105**, 017802 (2010).
- [17] L. Kong, X. Wu, and R. Car, *Phys. Rev. B* **86**, 134203 (2012).
- [18] N. Marzari, A. A. Mostofi, J. R. Yates, I. Souza, and D. Vanderbilt, *Rev. Mod. Phys.* **84**, 1419 (2012).
- [19] Z. Li, Ph.D. thesis, Physics Department, Princeton University, 2012.
- [20] J. P. Perdew, K. Burke, and M. Ernzerhof, *Phys. Rev. Lett.* **77**, 3865 (1996).
- [21] P. Giannozzi, P. Baroni, N. Bonini, M. Calandra, R. Car, C. Cavazzoni, D. Ceresoli, G. L. Chiarotti, M. Cococcioni, and I. Dabo, *J. Phys. Condens. Matter.* **21**, 395502 (2005).
- [22] Individual IPs were calculated by projecting the QWs on to a real-space sphere of 1.5 Å [9] centered on the O\* atom while in a stable complex and centered on the transferring proton during PT [23]. The IPs of hydrated ions are amplified by a factor of 10 in order to increase their visibility. The identity of both the OH<sup>-</sup> and the H<sub>3</sub>O<sup>+</sup> are determined by counting the number of H<sup>+</sup> inside a covalent radius of 1.17 Å for each oxygen atom in a given configuration. Those oxygens containing one or 3 H atoms within their covalent radius are referred to as O\* and determine both OH<sup>-</sup> and H<sub>3</sub>O<sup>+</sup> respectively.
- [23] Configurations are considered to be in a Proton transfer event when a single H<sup>+</sup> could not be associated with any oxygen molecules, in accordance with Ref. [22].
- [24] B. Kirchner, *Chem. Phys. Chem.* **8**, 41 (2007).
- [25] D. Prenergast, J. Grossman, and G. Galli, *J. Chem. Phys.* **123**, 014501 (2005).
- [26]  $\delta$  is defined as  $\delta = |R_{O^*H} - R_{O_wH}|$ , where  $R_{O^*H}$  and  $R_{O_wH}$  are the distances between a shared proton and O\* [22] or a surrounding water molecule's oxygen, respectively. The minimum  $\delta$  value for a particular O\* is considered most likely to produce a PT, and  $\delta = 0$  indicates that the shared proton is halfway between two molecules [2].
- [27] D. Marx, M. Tuckerman, J. Hutter, and M. Parrinello, *Nature* **397**, 601 (1999).
- [28] C. Zhang, and J. Wu, G. Galli, and F. Gygi, *J. Chem. Theory Comp.* **7**, 3054 (2011).
- [29] B. Santra, J. Klimeš, D. Alfé, A. Tkatchenko, Ben Slater, A. Michaelides, R. Car, and M. Scheffler, *Phys. Rev. Lett.* **107**, 185701 (2011).
- [30] R. A. DiStasio, O. Anatole von Lilienfeld, and A. Tkatchenko, *Proc. Natl. Acad. Sci.* **109**, 14791 (2012).
- [31] C. Zhang, T. A. Pham, F. Gygi, and G. Galli, *J. Chem. Phys.* **109**, 14791 (2013).
- [32] C. Zhang, D. Donadio, F. Gygi, and G. Galli, *J. Chem. Theory Comput.* **7**, 1443 (2011).
- [33] W. Kang and M. S. Hybertsen, *Phys. Rev. B* **82**, 195108 (2010).
- [34] D. Lu, F. Gygi, and G. Galli, *Phys. Rev. Lett.*, **100**, 147601 (2008).
- [35] The static GW is found to slightly overestimate the IP [13, 33], which can be corrected by frequency dependence in GW method.